Sputter Profiling Through Ni/Fe Interfaces by Auger Electron Spectroscopy

Abstract: Sputter characteristics of nickel-iron systems in the form of layer interfaces and bulk alloy films have been studied by Auger electron spectroscopy. The sputter rates for pure nickel and iron and their alloys have been determined and are independent (within 10%) of the grain size and film composition. The various factors that contribute to the broadening of depth profiles have been examined. The initial broadening of 4.5 nm at zero overlayer thickness is mainly attributed to the effects of electron escape depth and compositional mixing due to ion bombardment. For thin films, the depth-dependent broadening induced by sputter damage has an approximately exponential dependence on the overlayer thickness. For thick films, this broadening is estimated to be about 10% of the sputter distance. The effect of ion-induced surface compositional mixing as a function of incident Ar⁺ ion energy has been studied by taking advantage of the different sampling depths of low and high energy Auger electrons.

Introduction

Microsectioning by ion bombardment, in conjunction with a surface analysis method like Auger electron spectroscopy (AES) or x-ray photoemission (XPS), provides a convenient and increasingly used tool for compositional profiling [1-4], although it must in general be considered a very destructive method. The impinging rare gas ions can cause selective sputtering [5–7]; surface atomic implantation ("knock-on") and radiation-enhanced diffusion [8-10], leading to compositional mixing [11, 12]; surface roughening [13, 14] and cratering, etc. Extended reviews of such effects are given by Coburn [4, 15] and Carter and Colligon [16]. These effects depend on the composition, the grain size, and the purity of the bombarded materials, as well as on the energy and type of ionic species, the current density, and the angle of incidence of the incoming ion beam. Furthermore, the results are known to be affected by target temperature [17] and by whether or not ion bombardment and AES measurement (electron beam irradiation) occur simultaneously [18]. When AES or XPS is used for surface analysis, additional broadening of the composition profile can arise from the finite sampling depth of the escaping electrons. Thus, in compositional profiling, the various effects must be evaluated before meaningful physical parameters can be extracted. In addition to theoretical investigations of sputtering [10, 19-21], recent publications describe empirical approaches to understanding the effects of ion bombardment on solid surfaces [11, 12, 22-25]. Coburn [22], Ho [23], and their coworkers have clearly demonstrated that surface roughness increases with an increase in sputter time. Pellerin et al. [24] have established that the depth distribution of ion-induced roughness on sapphire surfaces is Gaussian-like, and Hofmann [25] has found that the depth profile of a Au-Cu layer has a Gaussian distribution. The effects of compositional mixing by impinging ions have been studied by McHugh [11], Ishitani et al. [12], and others [15]. Compositional profiling within the first 2–3 nm with both low and high energy electrons has been frequently used to study surface enrichment in alloys [26, 27].

Our interest in sputtering behavior originated from our study of the interdiffusion of Ni-Fe bilayers [28]. In this paper we report the results of both depth-dependent and depth-independent broadening of Ni-Fe interfaces by Ar⁺ ion bombardment. In particular, by utilizing both high and low energy Auger electrons with different sampling depths, we have determined the relative sputter rates for high-purity iron and nickel, and FeNi alloys; the extent of surface roughening as a function of sputter time; and the effect of the ion-induced compositional mixing in the altered surface layers.

Experimental procedure

All experiments were carried out in a PHI ESCA and Auger spectrometer (Model 548) at a base pressure of $\leq 1.33 \times 10^{-8}$ Pa (1 Pa = 7.52×10^{-3} torr) with a standard bell jar

Copyright 1978 by International Business Machines Corporation. Copying is permitted without payment of royalty provided that (1) each reproduction is done without alteration and (2) the *Journal* reference and IBM copyright notice are included on the first page. The title and abstract may be used without further permission in computer-based and other information-service systems. Permission to republish other excerpts should be obtained from the Editor.

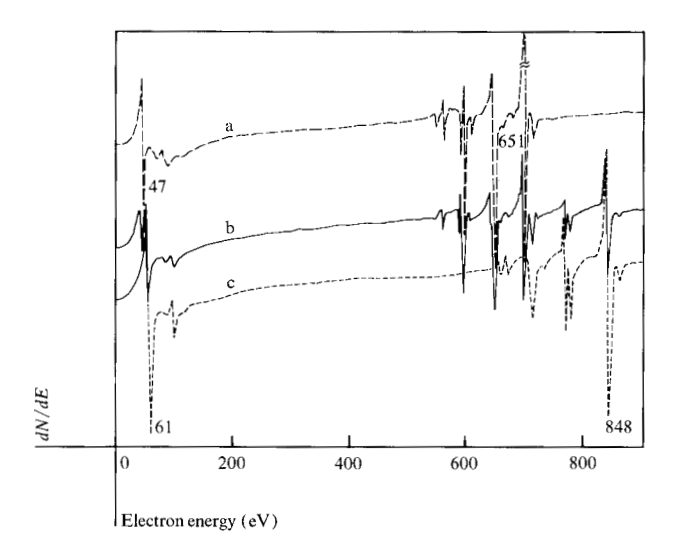
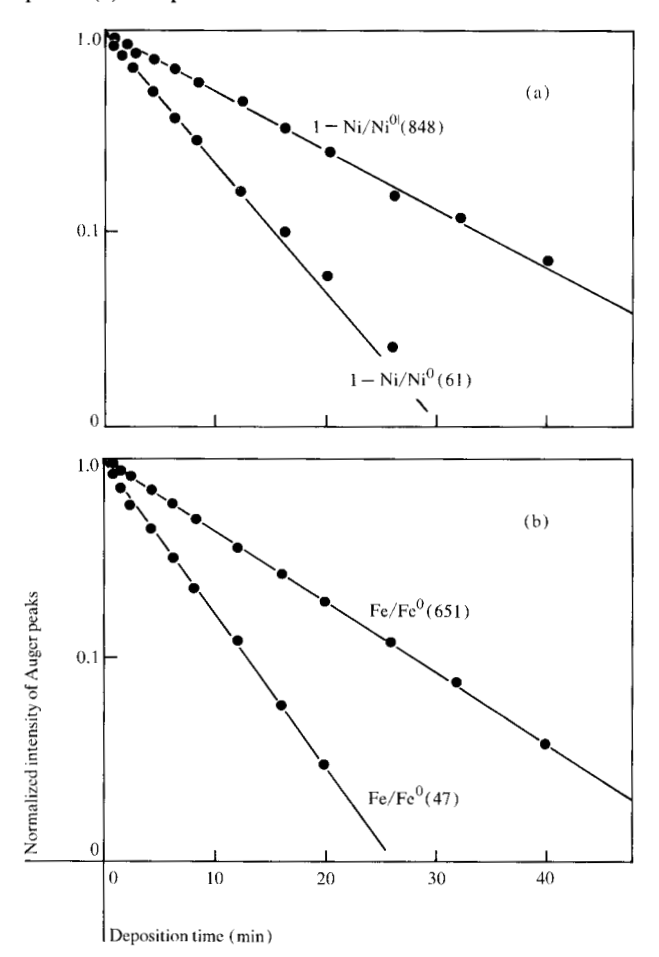


Figure 1 Auger spectra for (a) the pure Fe substrate, (b) some Ni on Fe, and (c) the pure Ni overlayer.

Figure 2 Normalized Auger intensities (relative to the appropriate pure metal peaks, Ni^0 or Fe^0 , as shown) for Ni deposited on Fe in situ as a function of film deposition time. (a) Nickel peaks: (b) iron peaks.



and a double-pass cylindrical mirror analyzer (CMA) with a concentric electron gun, an ion gun (PHI Model 04-161), and an in situ nickel evaporation source. The substrate, a polycrystalline iron foil (ROC/RIC, 99.99% purity 8-mm dia × 0.25-mm thickness), was held by a Varian manipulator that allowed for heating and liquid nitrogen cooling of the sample. In order to reduce the effect of continuous electron-beam irradiation on the surface composition, ion bombardment and AES detection were not carried out simultaneously. For the same reason, both the electron beam and the ion beam were defocused to reduce beam densities. A 5-µA electron beam was used for AES excitation. The angles between the normal of the sample surface and the axis of CMA, and the ion beam were 30° and 45°, respectively. For all profile measurements the Ar^{+} ion beam current was held at 11 μA (Ar pressure of 6 \times 10⁻³ Pa). Except for the study of the effect of ion energy (0.5-2.0 keV) on surface compositional mixing, the beam voltage was set at 1 keV. The sputter rate was determined from time required to sputter through nickel and iron films of known thickness (measured with a laser interferometer). Relative sputter rates for pure nickel, iron, and Ni/Fe alloy films were also determined by the weight losses due to ion bombardment, by using a balance sensitive to 1 μ g.

The sample temperatures were measured with a chromelalumel thermocouple spot-welded to the edge of the iron foil. The *in situ* Ni evaporation source, consisting of coils of tungsten wire wrapped with high-purity Ni wire (99.999%, 0.25-mm dia), was shielded with a stainless steel tube. A constant evaporation rate of 0.1-0.5 nm/min could be obtained by applying the appropriate power to the tungsten coil. The iron foil was cleaned by repetitive Ar⁺ bombardment at 1073 K and 623 K. This treatment removed traces of S, N, O, Cl, P, and C.

Prior to each film deposition, the nickel wire was properly outgassed, and the iron foil was sputtered clean at room temperature and subsequently annealed at 773 K for 20 min. The Fe substrate was cooled to ≈123 K with liquid nitrogen and then Ni was evaporated onto the substrate. During sputter profiling, the sample was rotated back and forth between the sputter ion gun and the cylindrical mirror analyzer positions. All profiling measurements were carried out at room temperature.

Two types of metal films were used in this study. Films evaporated in situ at low temperatures were used for all profiling measurements and interdiffusion studies [28]; some films prepared in this manner were also used for determining sputter rates. These films had an average grain size of about 30 nm. The second type of film, prepared by e-beam deposition in a separate vacuum chamber at high deposition rate (150 nm/min) and at room temperature or slightly higher, had a grain size of about 1 μ m. These films were only used in determining the relative

sputter rates. The surface topography and grain size were determined by both scanning- and transmission-electron microscopy (SEM and TEM).

Results and discussion

• Sputter rates and escape depths of Auger electrons Figure 1 shows the typical Auger spectra of Ni evaporated onto Fe foil. The normalized peak-to-peak heights of the Auger iron peaks (47 and 651 eV) [Fig. 2(b)] and nickel peaks (61 and 848 eV) [Fig. 2(a)] are taken to be proportional to their concentrations. (For the Fe/Ni system, calibration of the signal vs composition is reasonably linear.) These peak height changes are shown in Fig. 2 as a function of deposition time. For normalization, the respective peak heights of pure Ni and Fe are always taken from the same experimental run so that the error induced by the variation in peak heights of the pure elements is reduced. Under our operating conditions the sputter rate with 1-keV Ar⁺ ions was determined to be 0.45 nm/min (±10%) for pure iron and nickel films and Ni/Fe multilayers of known thickness. The sputter rates for Ni and Fe are approximately the same (that for Ni is at most only 10% greater); there is no significant effect of selective sputtering. We have further confirmed these relative sputter rates by bombarding films of pure Ni and Fe, and the alloys (compositions in atomic percent given parenthetically) Ni(80)Fe(20), Ni(50)Fe(50), Ni(20)Fe(80) with 1keV Ar+ ions and measuring their weight losses. For weight losses up to 100 μ g, the sputter rates were again found to be constant to within $\pm 10\%$, with Ni having a tendency toward a slightly higher sputter rate. Laegreid and Wehner [29] have determined sputter yields of 1.52 and 1.26 by using 0.6-keV Ar⁺ ions for Ni and Fe, respectively. Carter and Colligon [16] have reported respective yields of 2.21 and 1.33 with 1-keV Ar⁺ ions. Since sputter yields are affected by the ion angle of incidence, the specimen purity, and the presence of background residual gases, the difference between our observed relative sputter yields and those reported by Laegreid, Carter, and their coworkers [16, 29] may be due to these factors. The effect of bombardment time on our sputter rate is unimportant (a decrease of <15% in 15 hours). To evaluate the effect of grain structure on the sputter rate, we have compared the etch rates of films prepared in situ (grain size ≈ 30 nm) to the rates of films prepared by e-beam deposition, (grain size ≈1000 nm), as characterized above. The sputter rates of the latter films are only slightly lower $(\approx 15\%)$ than those for films of smaller grain size. This observation (that the grain size has little effect on sputter rate) is consistent with the fact that films of known thickness, which have been annealed at various temperatures up to 773 K [28], show very similar sputter rates. Fur-

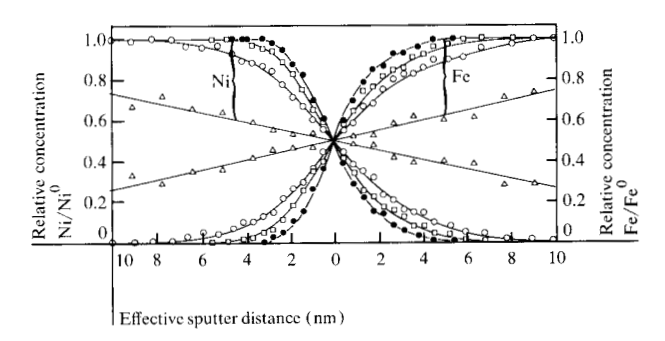


Figure 3 Depth profiles for Ni/Fe at room temperature as a function of overlayer Ni thickness (in nm): \bullet , 6; \Box , 20; \bigcirc , 73; and \triangle , 485. Curves marked Ni or Fe are for the respective Auger lines. Effective (relative to the clean Fe substrate surface) sputter distance to the right of 0 is toward (into) the Fe substrate, while distance to the left is away from the Fe substrate.

Fig. 3) are reasonably symmetrical with respect to the metallic interface, which indicates that the sputter rate does not depend significantly on the grain size (expected to be quite different for the deposited Ni overlayer and the polycrystalline Fe substrate). We conclude that neither the elemental composition nor the grain structure exerts a strong influence on the sputter rate of Ni and Fe under our experimental conditions.

Having established a sputter rate for iron and nickel, we were able to determine the thickness of films deposited *in situ* from the time required to sputter to the center point of the depth profile (Fig. 3). By using this film thickness we can calculate the *in situ* Ni evaporation rate and obtain the escape depths of Ni and Fe Auger electrons through the Ni overlayer. Figure 2 shows the attenuation of Fe signals and the increase of Ni peaks as Ni is deposited on Fe. The peak heights obey the exponential relations [30]

$$I_{\rm s} = \exp(-x/0.75\lambda_{\rm Fe})$$
 for the Fe substrate, (1)

 $I_{\rm c}=1-\exp{(-x/0.75\lambda_{\rm Ni})}$ for the Ni condensate, (2) and

$$x = Rt, (3)$$

where I_s and I_c are the normalized peak-to-peak heights of Fe and Ni peaks, the subscripts s and c refer to substrate and condensate, respectively, x is the thickness of the Ni overlayer, R and t are the evaporation rate and time, and $\lambda_{\rm Fe}$ and $\lambda_{\rm Ni}$ are the escape depths of the respective Auger electrons. The factor 0.75 arises from the detecting geometry of the cylindrical mirror analyzer. From our sputter rate of 0.45 nm/min at an ion energy of 1 keV, we have determined that R=0.1–0.5 nm/min (constant for any given deposition), and that $\lambda(47$ and 61 eV) = 0.5 nm, $\lambda(651 \text{ eV})=1.1 \text{ nm}$, and $\lambda(848 \text{ eV})=1.35 \text{ nm}$. These escape depths are in good agreement with the "universal"

thermore, depth profiles through the Ni-Fe layers (see

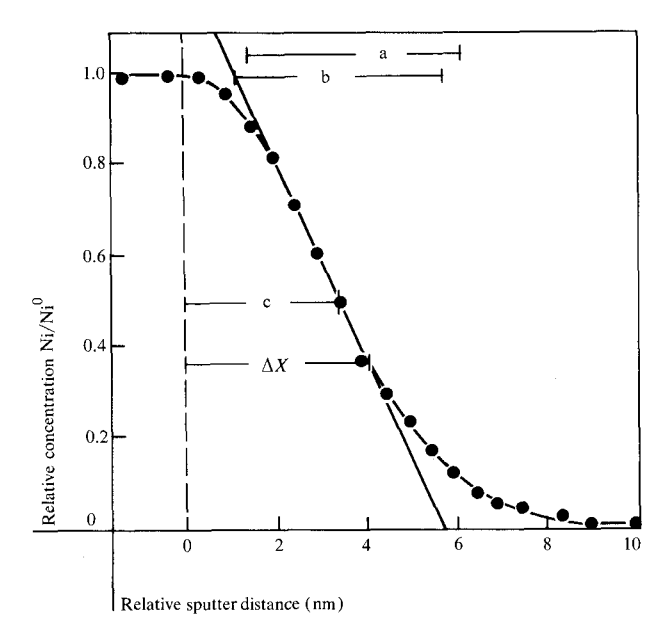


Figure 4 Various definitions of the interface width: (a) 90% to 10% by Coburn et al. [22], (b) present study, (c) half of full width at the half maximum by Ho and Lewis [23]. Data points are the measured depth profile for a 6-nm film on Fe. The curve tracing the dots is a calculated Gaussian with Δx , while the straight line is the slope at the interface (relative concentration = 0.5; concentrations are derived from normalized peak-to-peak heights of Auger lines, as discussed in the text).

curve" that describes the energy dependence of the mean free path of electrons in metals [31, 32]. The exponential dependence shown in Fig. 2 also indicates that the Ni overlayer is deposited homogeneously on top of the Fe substrate. This is opposed, for instance, to island growth behavior, which would not follow a simple exponential relationship. In turn, the measured escape depths enable us to control the thickness of the metal film deposited in situ.

• Intrinsic and ion-induced broadening of depth profiles
Any real bilayer interface deviates from the ideal steplike
compositional distribution. Even if an ideal microsectioning technique were available such that material
could be removed layer by layer without perturbing its
composition and structure, there are intrinsic factors that
could contribute to the broadening of a composition profile: thickness variations in the original film, initial interdiffusion, and, if AES is used for profiling, the finite sampling depth of Auger electrons. From our Ni-Fe interdiffusion studies [28], we have found that interdiffusion at
or below room temperature is negligible. Escape depths
of Auger electrons contribute less than 2.7 nm to the observed initial broadening of 4.5 nm (discussed below). Ion
bombardment causes further broadening of the depth pro-

files. The broadening due to ion-induced mixing and diffusion is expected to be relatively independent of the depth of analysis, whereas surface roughening and cratering can cause the broadening to increase as the total depth of analysis increases [22, 23]. Following the method of Coburn et al. [22], we have divided these intrinsic and bombardment-induced effects into two categories, namely, depth-dependent and depth-independent effects.

Before further evaluation, a discussion of the definition of the width of the depth profile is in order. Some workers define the width of the interface by the sputter time (or distance) required for the elemental signal to decrease from 0.9 to 0.1 [22], whereas some use the interval between 0.84 and 0.16 [33]. Others describe the broadening in terms of the resolution function and express the interface width in terms of the full width at the half maximum (FWHM) of this function [23]. We prefer to define the interface width by the absolute value of the inverse of the slope (or the tangent) at an elemental signal of 0.5. We have chosen this definition from the consideration that for interdiffusion of solids (a major application of sputter profiling) following Fick's laws, the concentration gradient due to diffusion is a Gaussian function, and the derivative at the interface is simply related to the diffusion constant by [28, 34]

$$S = -0.5/(\pi Dt)^{1/2},\tag{4}$$

where S is the slope or the first derivative of the depth profile at the interface, and D and t are the diffusion constant and the diffusion time, respectively. Thus, if an observed profile is due to contributions from the diffusion process and the intrinsic and sputter-induced broadening mentioned above, the diffusion constant D can be obtained by simply measuring the interface slopes at t = 0and after some diffusion time t. Our diffusion studies will be discussed in detail elsewhere [28]. It is instructive to compare these various definitions of interface width. We and other workers [25] have found that, in general, the concentration profile of a thin film is close to a Gaussian function. A typical profile (in comparison with a Gaussian function) and the various definitions of interface width are shown in Fig. 4. If the depth profile is assumed to be a Gaussian function characterized by Δx , it follows that

$$Y = \exp{(-x^2/\Delta x^2)},$$
 $\Delta W \equiv x_1(Y_1) - x_2(Y_2),$
 $\Delta W(0.1-0.9) = 1.193\Delta x,$ (Coburn et al. [22])
 $\Delta W(0.16-0.84) = 0.936\Delta x,$ (Honig and Harrington [33])
 $\Delta W(\text{FWHM}) = 1.667\Delta x,$ (Ho and Lewis [23])
and
 $\Delta W \equiv |1/S| = 1.201\Delta x,$ (present study)

where Y is the elemental concentration, x is the distance, and ΔW is the interface width as defined by the various groups. If the Gaussian assumption is reasonable, the values of the interface widths reported by the various studies can be correlated by these equations.

The interface widths ΔW measured with Ni(848-eV) profiles vs film thickness W for various Ni/Fe layers are plotted in Fig. 5. We note that ΔW has an approximately exponential dependence on film thickness, except for films thicker than 300 nm. Here, W is defined as the distance between the original film surface and the observed metallic interface (elemental signal = 0.5). Ho and Lewis [23] have studied the Ag/Au and Cu/Ni systems. Replotting their data in the same way, we find that the Ag/Au results show an exponential dependence, whereas the Cu/Ni data are almost linear. Hofmann [25] has suggested a square-root dependence in his analysis of Au/Cu results. A theoretical understanding of this problem is still lacking; however, knowledge of this relationship is very important when computing sputter profiles.

As ΔW is extrapolated to a zero overlayer thickness, we obtain an initial broadening of 4.5 nm. For a steplike interface, it can readily be shown that the finite sampling depth of the Auger electron can broaden the interface width to twice the value of the electron escape depth (λ is 1.35 nm for the 848-eV electrons, and 0.5 nm for the 50-eV electrons). This is the maximum contribution of the electron escape depth to the initial broadening. Further broadening can arise from both variations in the overlayer thickness and ion-induced compositional mixing at early stages of ion bombardment. Variations in the overlayer thickness are caused by roughness of the initial substrate surface and damaging effects of ion bombardment. As mentioned before, our Ni film is deposited homogeneously on top of the Fe substrate (Fig. 2); thus, the thin overlayer should replicate the initial substrate roughness. For very thin films at the beginning of ion bombardment, the ion-induced surface roughness should be quite negligible. Hence, even though the true bilayer interface is not a plane, it still acts as a concentration step, because both deposition and sputter removal of the nickel overlayer replicate the original substrate surface topography. Therefore, we tend to believe that compositional mixing and the effect of the electron escape depth are the major factors contributing to the observed initial interface broadening.

To assess the depth-dependent effects, we plotted $\Delta W/W$ vs W (Fig. 6). The ratio $\Delta W/W$ drops rapidly within the first 20 nm and reaches 0.1 at 60 nm, and then remains nearly constant for films up to 500 nm thick. Thus, for films over 60 nm thick, the observed profile broadening is mainly due to bombardment damage (such as surface roughening and cratering), and this broadening is about 10 percent of the film thickness for our Ni/Fe

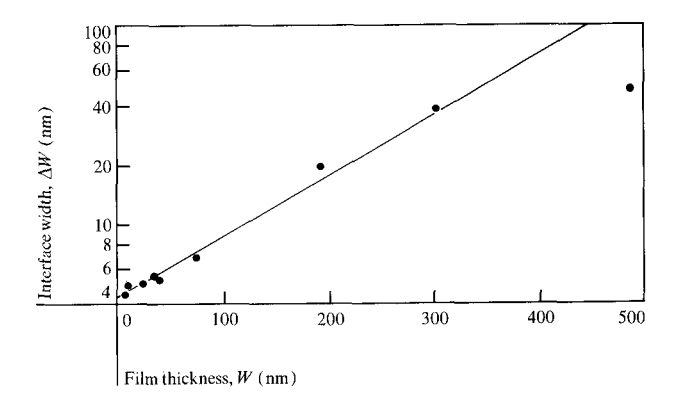


Figure 5 Interface width as a function of the film thickness for various Ni/Fe films.

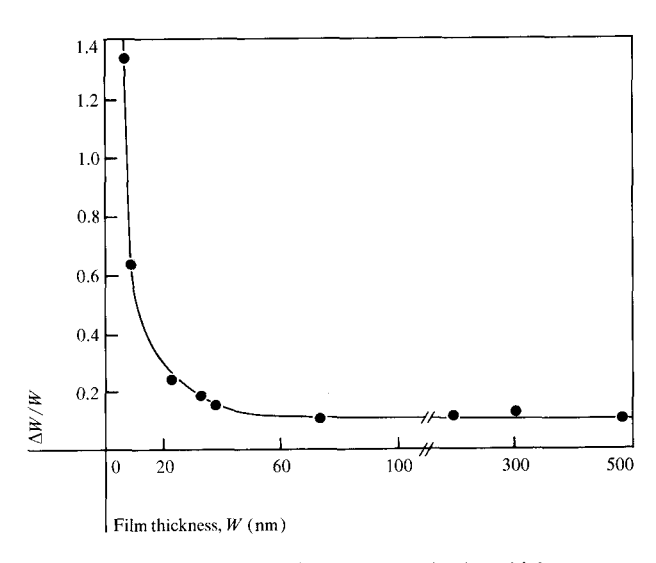


Figure 6 Ratio of the interface width to the film thickness as a function of film thickness.

interface. Previously reported values for profile broadening have varied from 14% for Ag/Au [23] and 2-8% for Cu/Ni [22, 23] to 6-10% for Au/Ni [35].

• Ion-induced surface compositional mixing

The importance of the surface compositional mixing due to momentum-induced atomic motion ("knock on") and ion-induced interdiffusion is well recognized from both theoretical and experimental considerations [8–10]. However, little work has been done to measure the thickness of the "altered layer" and the extent of compositional mixing within this layer. McHugh [11] has studied atomic mixing in the subsurface region of Ta₂O₅ films with secondary ion mass spectrometry (SIMS). Chu et al. [8] and Liau et al. [9] have applied Rutherford backscattering

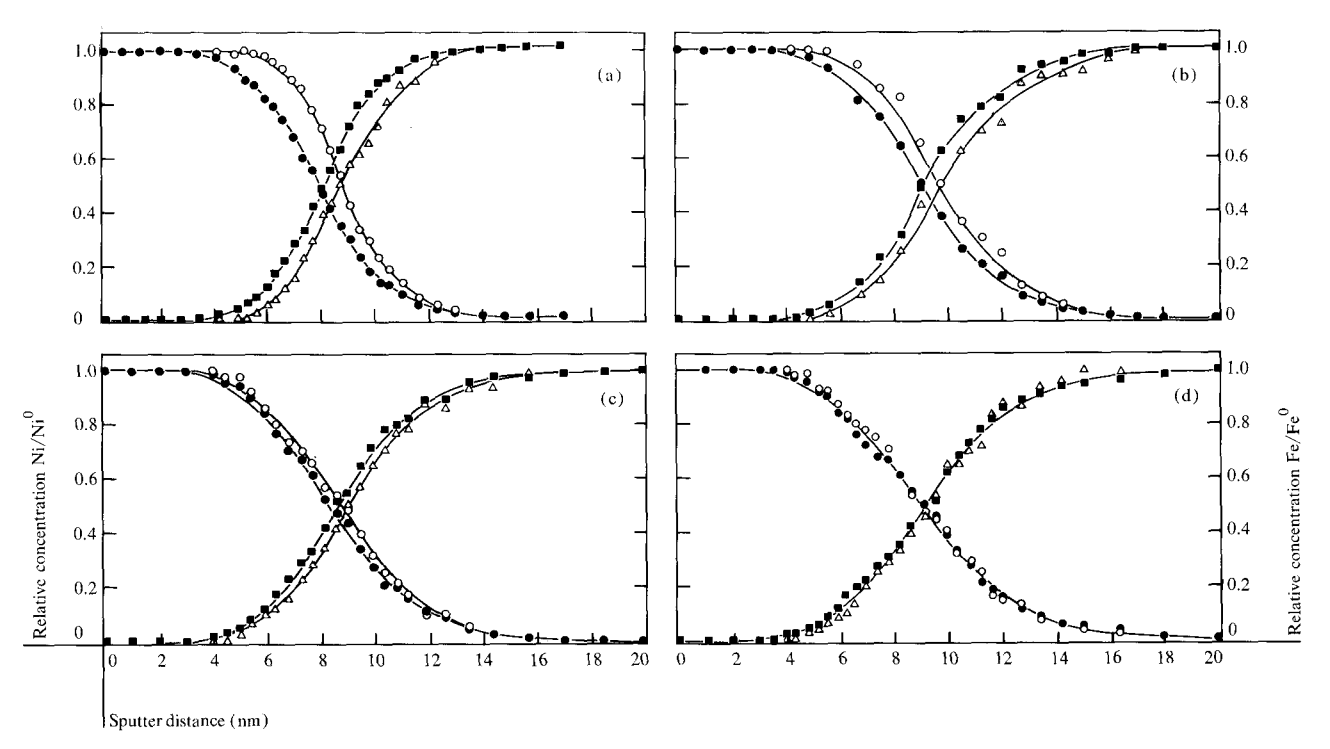


Figure 7 Depth profiles derived from the different Auger peaks (eV): \bullet Ni(848), \bigcirc Ni(61), \blacksquare Fe(651), and \triangle Fe(47) for an 8-nm Ni film on Fe bombarded by Ar⁺ ions of various energies (keV); (a) 0.5, (b) 1.0, (c) 1.5, and (d) 2.0.

techniques to a number of binary alloys in order to examine surface compositional changes due to ion bombardment. The subject of the "altered layer" has also been considered by Ishitani et al. [12], Winters [36], Ho [6], and others [15].

We have used the property that Auger electrons of different kinetic energies monitor different sample depths from the surface to study the effect of ion bombardment on the Ni/Fe surface. If the thickness of the altered layer is much greater than the escape depth of high energy Auger electrons and if the compositional mixing is fairly uniform within this layer, the depth profile measured by the low energy Auger peaks [Fe(47 eV) and Ni(61 eV)] should be the same as that given by the high energy Auger peaks [Fe(651 eV) and Ni(848 eV)]. However, if the thickness of the altered layer is small compared with the escape depths of high energy electrons, then the Ni and Fe low energy profiles should be shifted away from the corresponding high energy profiles. The direction of this shift should be away from the surface, i.e., toward a greater sputter distance. Since the extent of surface mixing depends on the penetration range of the impinging ions, both the shapes of the depth profiles measured with high and low energy electrons and the separation of these profiles should also change as the ion energy is varied. Figures 7(a)-(d) show the depth profiles of 9-nm Ni films on Fe (with high and low energy Auger peaks) as

a function of Ar⁺ ion energy in the range of 0.5 to 2.0 keV. The effect of ion energy on the depth profiles is clearly evident. For ion energies below 2 keV, the measured low energy profiles are shifted toward a greater sputter distance with respect to the high energy profiles. With 500-eV Ar⁺ ion energy, the separation between the cross point of the Ni and Fe high energy profiles and the cross point of the corresponding low energy profiles is about 0.8 nm. This separation decreases from about 0.7 nm at 1 keV to 0.4 nm at 1.5 keV, while at 2 keV ion energy the profiles almost coincide. It is clear that substantial compositional mixing of Ni and Fe has occurred in the surface region bombarded by 2-keV ions, and that the elemental composition within the sampled layer must be rather uniform in depth. In this case, the thickness of the altered layer must be equal to or greater than the sampling depth of the high energy Auger electrons. At the lower ion energies, compositional mixing is less complete, because the low and high energy Auger electrons obviously probe different compositions. We have performed model calculations of compositional mixing at the metallic interface induced by ion bombardment using a steplike interface. The extent of in-depth compositional mixing is considered by using several broadening functions. Depth profiles are then calculated by convolution of the broadened profile due to mixing with the Auger electron escape depth. Details of these calculations will appear later [37]. It suffices to mention that calculated profiles obtained by using mixing depths of the order of 1.5–4.0 nm with 0.5–1:5-keV ions and 4.0 nm or greater with 2-keV ions agree reasonably well with the experimentally measured profiles. These values seem to be reasonable in comparison with previous studies of other metal systems [4, 36].

Investigations of the surface compositional mixing effect have been carried out deliberately with very thin films (9-10 nm) in order to minimize the bombardmentinduced roughening effect shown in Fig. 5. Superposition of crater roughness could play a complex role, possibly obscuring the pure compositional mixing effect, although the general belief is that ion-induced surface mixing is independent of the depth of analysis [22]. Figure 8 shows high and low energy profiles for a 74-nm Ni film on Fe using a 1.0-keV Ar⁺ ion beam. As expected, the depth profiles are broader than those of the 9-nm films [Fig. 7(b)]. Shifts of low energy profiles away from the high energy profiles are still observed, however, and this does indeed suggest that for both thick and thin films compositional mixing by 1.0-keV ions is incomplete within the altered layer, and that the mixing depth is not two or three times greater than the escape depth of the high energy Auger electrons.

Conclusion

We have determined the relative sputter rates of pure nickel and iron, and nickel-iron alloy films. It is observed that under our ion bombardment conditions and with 1-keV Ar⁺ ions, nickel is sputtered at about the same rate or only slightly faster than iron. The sputter rate is not significantly affected by either the alloy composition or the grain size of these films. Escape depths of Auger electrons are also determined for Ni films deposited on Fe. For depth profiling through Ni-Fe interfaces, the intrinsic and ion-induced broadening effects are examined. The interface width determined from the inverse of the slope at the profile interface is found to have an approximately exponential dependence for films up to 300 nm thick. The extrapolated finite interface width at zero overlayer thickness exceeds the sampling depth of the Auger electrons and is attributed to the effect of compositional mixing across the original metallic interface due to ion bombardment. The depth-dependent broadening is caused mainly by sputter damage such as surface roughening and cratering, and is estimated to be about ten percent of the overlayer thickness. The effects of ion-induced surface compositional mixing, including "knock-on" and radiationenhanced diffusion, are further studied by using both low and high energy Auger electrons that monitor different sample depths. We find that the extent of compositional mixing is of the order of the escape depth of 850-eV Auger electrons for Ar⁺ ion energies of 0.5 to 1.0 keV, but equal

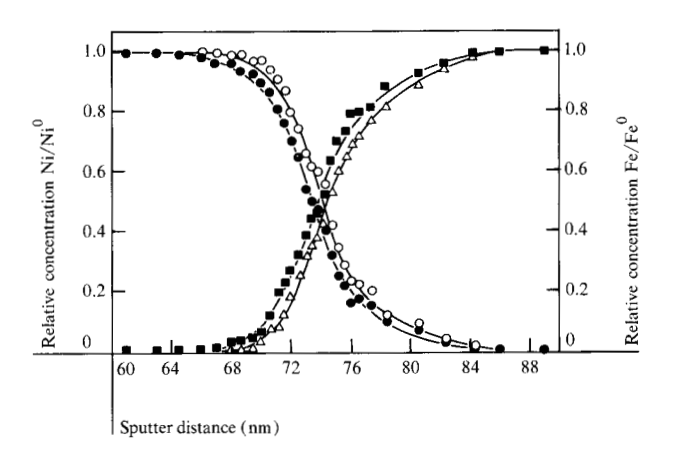


Figure 8 Depth profiles derived from the different Auger peaks (eV) for a 74-nm Ni film on Fe bombarded by 1.0-keV Ar^+ ions: \bullet Ni(848), \bigcirc Ni(61), \blacksquare Fe(651), and \triangle Fe(47).

to or greater than 4.0 nm for 2-keV ions. Our results also indicate that at these ion energies, under steady state conditions [38], surface mixing is quite insensitive to the sputter distance.

The method for using both low and high energy electrons, although frequently employed to study surface enrichment in alloys [26, 27], has been extended to depth profiling in order to gain physical insight into the effect of compositional mixing by ion bombardment. The method should have rather general applicability, as long as Auger peaks at different energies are available. For compositional profiling, our findings suggest that a combination of low energy ions (≤1 keV) for sputtering and low energy Auger electrons for surface analysis can come closest to giving a picture of the "true" interface gradient.

Acknowledgments

We are grateful for the SEM and TEM analyses performed by H. J. Arnal and R. H. Geiss. J. W. Coburn and H. F. Winters are thanked for many helpful discussions concerning aspects of ion bombardment of solids.

References and note

- 1. P. Palmberg, J. Vac. Sci. Technol. 9, 160 (1972).
- M. L. Tarng and G. K. Wehner, J. Appl. Phys. 42, 2449 (1971).
- 3. D. M. Halloway, J. Vac. Sci. Technol. 12, 392 (1975).
- J. W. Coburn and E. Kay, Crit. Rev. Solid State Sci. 4, 561 (1974), and references therein.
- H. Shimizu, M. Ono, and K. Nakayama, Surface Sci. 36, 817 (1973).
- P. S. Ho, J. E. Lewis, H. S. Wildman, and J. K. Howard, Surface Sci. 57, 393 (1976).
- 7. A. van Oostrom, J. Vac. Sci. Technol. 13, 224 (1976).
- 8. W. K. Chu, J. K. Howard, and R. F. Lever, J. Appl. Phys. 47, 4500 (1976).
- Z. L. Liau, W. L. Brown, R. Homer, and J. M. Poate, Appl. Phys. Lett. 30, 626 (1977).
- 10. P. K. Haff, Appl. Phys. Lett. 31, 259 (1977).

- 11. J. A. McHugh, Radiat. Eff. 21, 209 (1974).
- 12. T. Ishitani and R. Shimizu, Phys. Lett. A 46, 487 (1974).
- 13. P. H. Holloway, J. Electron Spectrosc. Relat. Phenom. 7, 215 (1975).
- 14. R. Shimizu, Jap. J. Appl. Phys. 13, 228 (1974).
- 15. J. W. Coburn, J. Vac. Sci. Technol. 13, 1037 (1976), and references therein.
- G. Carter and J. S. Colligon, Ion Bombardment of Solids, American Elsevier, New York, 1968, p. 310.
- 17. H. M. Windawi, Surface Sci. 55, 573 (1976).
- 18. T. Smith, Surface Sci. 55, 601 (1976).
- P. Sigmund, Phys. Rev. 184, 383 (1969); also, J. Mater. Sci. 8, 1545 (1973).
- H. F. Winters, Advances in Chemistry Series, R. J. Gould, ed., American Chemical Society, Washington, DC, 1976, Vol. 158, p. 1.
- 21. H. W. Pickering, J. Vac. Sci. Technol. 13, 618 (1976).
- J. W. Coburn, E. W. Eckstein, and E. Kay, J. Appl. Phys. 46, 2828 (1975).
- 23. P. S. Ho and J. E. Lewis, Surface Sci. 55, 335 (1976).
- 24. C. J. Pellerin, J. Christensen, R. C. Jerner, and J. H. Peavey, J. Vac. Sci. Technol. 12, 496 (1976).
- 25. S. Hofmann, Appl. Phys. 9, 59 (1976).
- 26. R. Bouwman and P. Biloen, Surface Sci. 41, 348 (1974).
- K. Watanabe, M. Hashiba, and T. Yamashina, *Surface Sci.* 61, 483 (1976).
- 28. T. J. Chuang and K. Wandelt, unpublished results.
- 29. N. Laegreid and G. K. Wehner, J. Appl. Phys. 32, 365 (1961).

- 30. M. P. Seah, Surface Sci. 32, 703 (1972).
- 31. C. J. Powell, Surface Sci. 44, 29 (1974).
- 32. I. Lindau and W. E. Spicer, J. Electron Spectrosc. Relat. Phenom. 3, 409 (1974).
- 33. R. E. Honig and W. L. Harrington, *Thin Solid Films* 19, 43 (1973).
- 34. P. M. Hall and J. M. Morabito, Surface Sci. 54, 79 (1976).
- 35. H. J. Mathieu, D. E. McClure, and D. Landolt, *Thin Solid Films* 38, 281 (1976).
- H. F. Winters and J. W. Coburn, Appl. Phys. Lett. 28, 176 (1976).
- 37. K. Wandelt and T. J. Chuang, unpublished results.
- 38. Since the sputter rates of Ni and Fe are found to be very similar, there is no transient state.

Received August 5, 1977; revised December 19, 1977

T. J. Chuang is located at the IBM Research Division laboratory, 5600 Cottle Road, San Jose, California 95193; the permanent address of K. Wandelt is Physikalisch-Chemisches Institut der Universität, Sophienstrasse 11, D-8000 Munich 2, West Germany.